한국표면공학회지
J. Kor. Inst. Surf. Eng.
Vol. 45, No. 6, 2012.
http://dx.doi.org/10.5695/JKISE.2012.45.6.242

<연구논문>

High Temperature Durability Amorphous ITO:Yb Films Deposited by Magnetron Co-Sputtering

Tae Dong Jung[a], Pung Keun Song[b*]

[a]National Core Research Center for Hybrid Materials Solution, Pusan National University, Busan 609-735, Korea
[b]Department of Materials Science and Engineering, Pusan National University, Busan 609-735, Korea

(Received December 29, 2012 ; revised December 29, 2012 ; accepted December 30, 2012)

Abstract

Yb-doped ITO (ITO:Yb) films were deposited on unheated non-alkali glass substrates by magnetron co-sputtering using two cathodes (DC, RF) equipped with the ITO and Yb_2O_3 target, respectively. The composition of the ITO:Yb films was controlled by adjusting the RF powers from 0 W to 480 W in 120 W steps with the DC power fixed at 70 W. The ITO:Yb films had a higher crystallization temperature (200ºC) than that of the ITO films (170ºC), which was attributed to both larger ionic radius of Yb^{3+} and higher bond enthalpy of Yb_2O_3, compared to ITO. This amorphous ITO:Yb film post-annealed at 170ºC showed a resistivity of 5.52×10^{-4} Ωcm, indicating that a introduction of Yb increased resistivity of the ITO film. However, these amorphous ITO:Yb films showed a high etching rate, fine pattering property, and a very smooth surface morphology above the crystallization temperature of the amorphous ITO films (about 170ºC). The transmittance of all films was >80% in the visible region.

Keywords: TCO, Yb-doped ITO, Amorphous ITO, Co-Sputtering

1. Introduction

Transparent conducting oxide (TCO) films are used widely in optoelectronic devices. In particular, indium tin oxide (ITO) films are used extensively as transparent conductive electrodes in multiple fields, such as liquid crystal displays (LCDs), plasma display panels (PDPs) and organic light emitting diodes (OLEDs) because they have high conductivity and transparency in the visible wavelength region[1-3]. However, polycrystalline ITO (c-ITO) films have some disadvantages, such as rough surface morphology and low etching rate[4]. Recently, with the advances in the flat panel displays (FPDs), there has been increasing demand for improvements in some of the critical properties of c-ITO films. In particular, despite the slightly higher resistivity, amorphous ITO (a-ITO) films are more attractive for FPDs applications than c-ITO films due to their excellent surface uniformity, high etching rate, good etchability and micro-patterning[5]. Some studies have examined the a-ITO deposition process through the injection of additional gas, control of the total gas pressure, or the addition of H_2O[5,6]. However, these methods deteriorate the electrical properties due to the decreasing carrier density and Hall mobility. The great part of the ITO films was produced by DC magnetron sputtering in the manufacturing line because this process has superior potential for the mass production. It is well known that film property is strongly dependent on the sintered target quality in magnetron sputtering. In addition, sintered ceramic target need to so many time to obtain high quality and optimum chemical composition in order to deposit a-ITO films without the need to control the deposition parameters. In our previous study, we confirmed that amorphous films (ITO:Ce, ITZO) showed very low surface roughness and good etchability[7-9]. Therefore, in this study, we tried to prepare Yb-doped ITO (ITO:Yb) films by magnetron co-sputtering using a Yb_2O_3 and ITO target because the ionic radius of

*Corresponding author. E-mail : pksong@pusan.ac.kr

Yb^{3+} (0.86 nm) is larger than that of In^{3+} (0.80 nm). In addition, higher bonding enthalpy of the Yb_2O_3 than In_2O_3 (Yb-O: 397 ± 17 KJ/mol, In-O: 320 ± 41.8 KJ/mol) can lead to a higher crystallization temperature than ITO films because the introduction of Yb atoms can deteriorate the crystallinity of ITO:Yb films. This study examined the effect of the Yb concentration on the structural and electrical properties of ITO:Yb films deposited by magnetron co-sputtering at room temperature and various annealing temperatures (170°C, 200°C).

2. Experimental Procedure

ITO:Yb films with thickness of 150-160 nm were deposited on unheated non alkali glass substrates (Corning 2000) by magnetron co-sputtering using two cathodes (DC,RF) at room temperature. The incident angle of the sputtered atoms to the substrate can be controlled by the setting angle of the two cathodes. The substrate was placed on the sample holder, which was separated by 60 mm and 95 mm from the center of the ITO and Yb_2O_3 targets, respectively. The Yb_2O_3 and ITO (10 wt.% SnO_2) targets were attached to the RF and DC cathodes, respectively. The composition of the ITO:Yb films was controlled by adjusting the RF power from 0 W to 480 W in 120 W steps with the DC power fixed at 70 W. The as-deposited films were post-annealed at various temperatures (170°C, 200°C) in a pure Ar gas atmosphere at 1.0 Pa for 60 min. The total gas pressure was kept at 0.5 Pa. All the targets were pre-sputtered for 5 minutes to obtain high reproducibility of the films prior to deposition. The chemical composition of the film was investigated using inductively coupled plasma (ICP, IRIS-intrepid, Thermo Elemeta). The film thickness was determined using a spectral reflectometer (ST2000-DLXn, K-MAC). The resistivity, carrier density and Hall mobility at room temperature were measured by Hall effect measurements (HMS-3000, ECOPIA). Crystallinity of the films was estimated by X-ray diffraction (XRD) using CuKα radiation with 40 kV-40 mA (Bruker axs D8 Discover). The surface morphology and the optical transmittance were studied by an atomic force microscopy with non-contact mode (AFM, L-Trace II, Nano Navi) and a UV-Visible spectrophotometer (UV-1800, Shimadzu) in the wavelength range from 190 to 1100 nm, respectively. The etching test was carried out in an etchant (10% HCl) at room temperature. The etching rate was calculated from the change in film thickness. Comparison of chemical composition was carried out by energy dispersive X-ray spectroscopy (EDS, Horiba, 7395-H) with 15 kV-10 mA analysis for wet-etched films (ITO and ITO:Yb).

The etching thickness and mean surface roughness of the films were estimated at five different points to produce more accurate estimates of the etching rate and mean roughness[6].

3. Results and discussion

Fig. 1 shows the changes in Yb content of the film deposited at various RF powers. As shown in figure, the Yb content in the films increased from 0 at.% to 4.32 at.% with increasing RF power in the Yb_2O_3 target from 0 W to 480 W. It is confirmed that Yb content in the films can be controlled by increasing RF power in the Yb_2O_3 target.

Fig. 2 show XRD patterns of the ITO and ITO:Yb films deposited on unheated substrates at various RF powers and post-annealed at different temperatures, respectively. The ITO film post-annealed at 170°C had a polycrystalline structure with strong peaks for (222) plane and relatively weak peaks for (400) plane. The crystallization temperature of the ITO films was reported to be approximately 170°C[7]. The ITO:Yb films post-annealed at 170°C did not show peaks for (222) and (400), and were considered to be amorphous. The films crystallized when the annealing temperature (T_a) was increased to >170°C. This confirms that the ITO:Yb films have a higher crystallization temperature than ITO films. The formation of amorphous ITO:Yb after annealing at 170°C is believed to have been caused by the increase in Yb content with increasing RF power. This suggests that Yb^{3+} ions interfere with the grain growth of

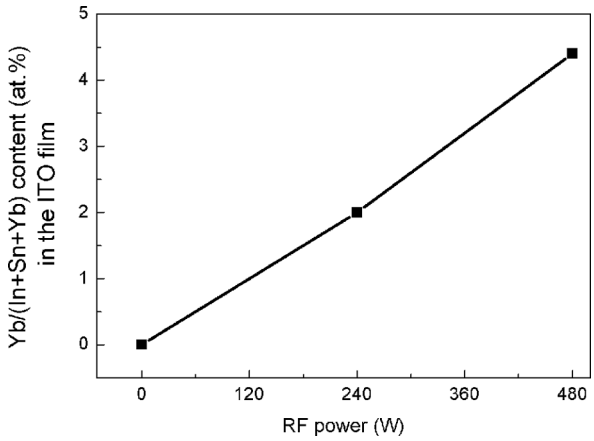

Fig. 1. Chemical composition of the films deposited with various RF power.

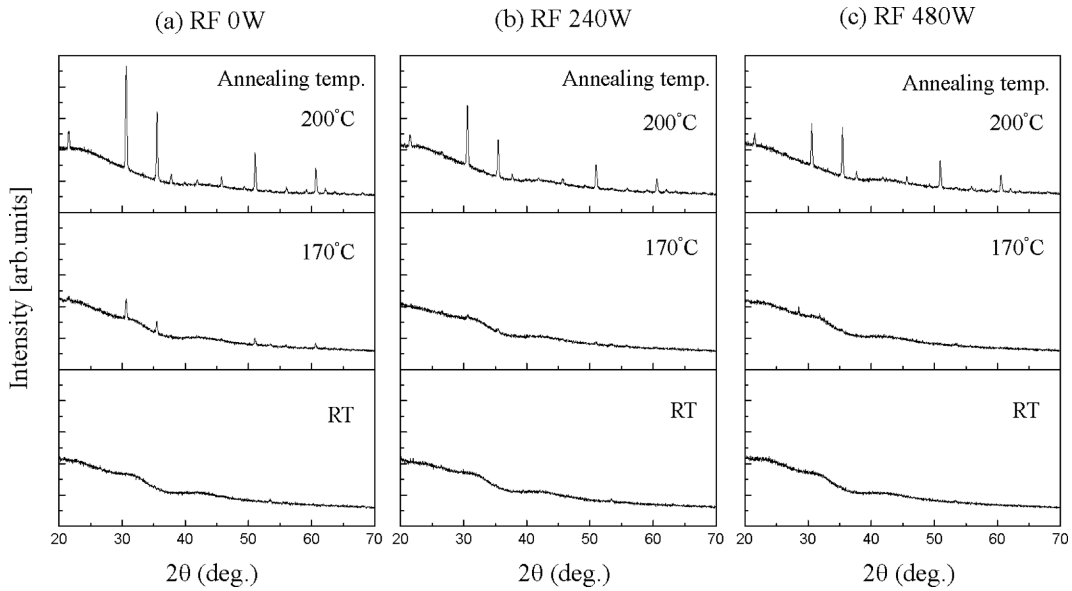

Fig. 2. XRD patterns of the ITO and ITO:Yb films deposited with the various RF powers at room temperature and post-annealed at different temperatures (170°C, 200°C).

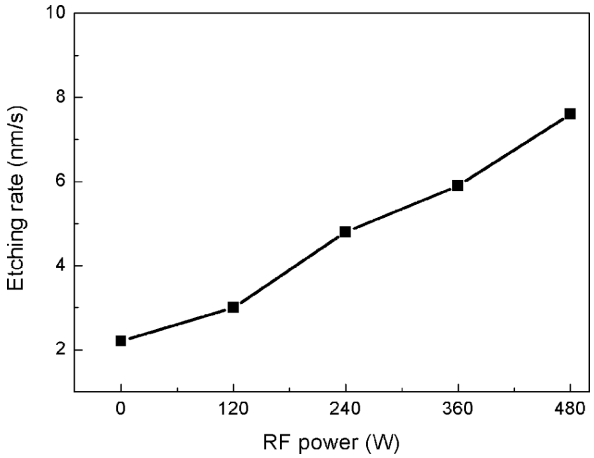

Fig. 3. Etching rates of ITO and ITO:Yb films post-annealed at 170°C.

ITO:Yb films on account of its larger ionic radius than In^{3+} ions, where ionic radiuses are 0.86 nm (Yb^{3+}) and 0.80 nm (In^{3+}), respectively. On the other hand, film crystllinity is also affected by the bond enthalpy of impurity ions. Bond enthalpy of Yb_2O_3 is higher than In_2O_3 (Yb-O: 397 ± 17 KJ/mol, In-O: 320 ± 41.8 KJ/mol). This means that an introduction of Yb atoms enhance the secondary nucleation density during the initial stage of film growth. Therefore, ITO:Yb films are expected to have a higher crystallization temperature than ITO films because the introduction of Yb atoms might deteriorate the crystallinity of ITO:Yb films. All the films were polycrystalline structure when post-annealed at 200°C. However, the ITO:Yb film deposited at RF power 480 W had a relatively weaker peak intensity than the other films post-annealed at 200°C.

Fig. 3 shows the etching rate as a function of the ITO and Yb content for ITO:Yb films post-annealed at 170°C. ITO films deposited at room temperature generally have a higher etching rate than those films deposited at high temperatures due to their amorphous structure[6,8,9]. In the case of the ITO:Yb films, the etching rate increased with increasing RF power. This might be due to the relatively small grain size of the ITO:Yb films caused by the interruption of grain growth as a result of the introduction of Yb atoms[8-10].

Fig. 4 show FESEM images of the etched (a) ITO and (b) ITO:Yb films post-annealed at 170°C. In the case of ITO film, the interface between the etched and non-etched film was quite rough. This can be explained by the crystallization of ITO films at 170°C. On the other hand, the ITO:Yb films had amorphous structure after annealing at 170°C. Therefore the interface between the etched and non-etched film was quite smooth and fine. This observation corresponds to the XRD patterns shown in Fig. 2. From Fig. 4 (a), A (white spot) is expected to show crystallites of ITO[4]. In order to accurate analyze, we investigated using EDS line profile. Figs. 4(c) and (d) show the EDS line profile images of A and B in Figs. 4(a) and (b). The diffraction of In (8.5 wt.%) was clearly observed in region A, but In was not observed in region B. The EDS line profile reveal that the white spot is a crystallite of ITO. The existence of crystallites

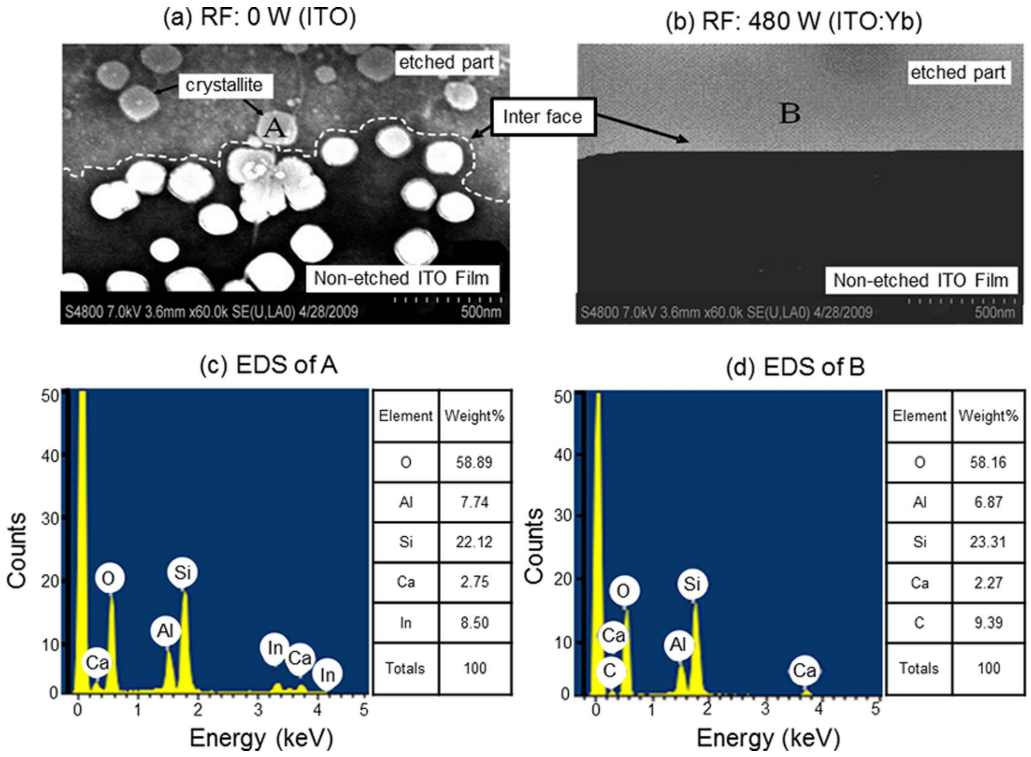

Fig. 4. FESEM images of the etched (a) ITO and (b) ITO:Yb (3.2 at.%) films post annealed at 170°C. The EDS line profile images of the (c) region A and (d) region B.

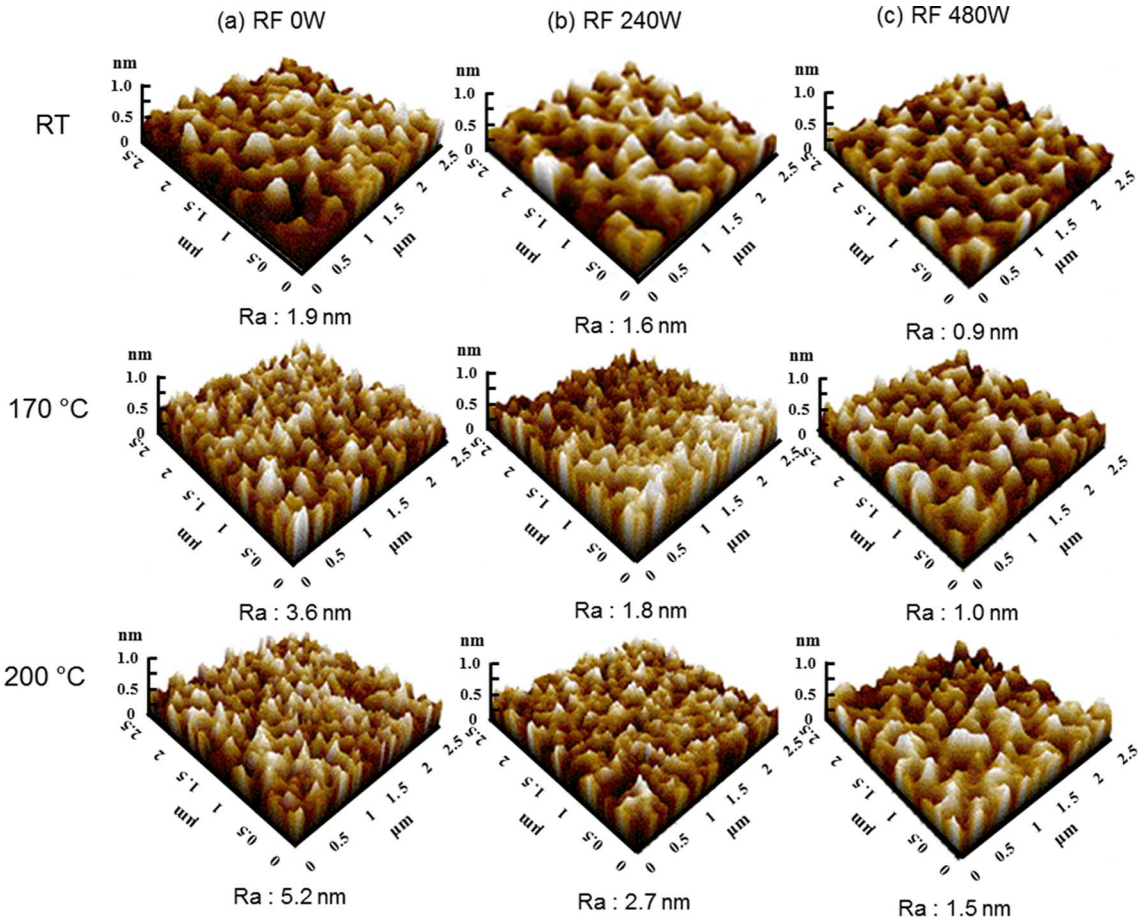

Fig. 5. AFM images of the ITO and ITO:Yb films deposited with the various RF powers [RF power: (a) 0 W, (b) 240 W and (c) 480 W] at room temperature and post-annealed at different temperatures (170°C, 200°C).

of ITO might be due to incomplete etching.

Fig. 5 shows AFM images of the ITO:Yb films at different annealing temperatures and RF powers supplied to the Yb_2O_3 target. The surface roughness of the films was quantified by the average surface roughness (R_a). The Ra of the ITO films increased with increasing T_a (1.9-5.2 nm). Although the Ra of the ITO:Yb films also increased with increasing T_a, the changes in R_a were smaller than its ITO films. In addition, AFM images showed that the R_a of all the films decreased with increasing RF power. The uniformity of all the films was improved by the introduction of Yb atoms, which was attributed to the suppression of grain growth with increasing Yb content in the ITO films[11,12]. From the above results, it was confirmed that the surface morphology of the ITO film was affected by the introduction of impurity atoms and T_a[8,10].

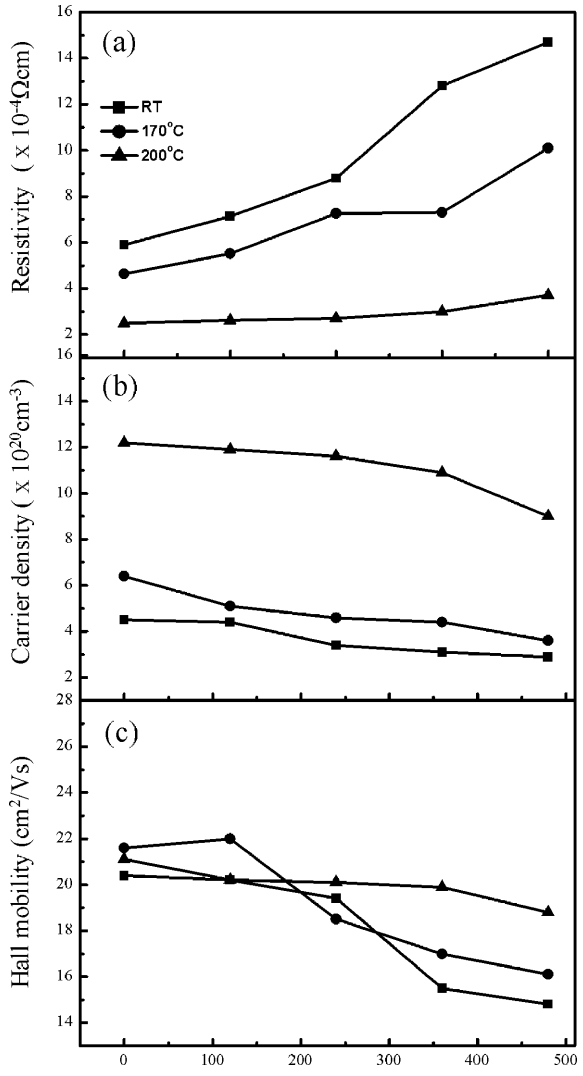

Fig. 6. (a) resistivity, (b) carrier density, (c) Hall mobility of the ITO and ITO:Yb films deposited with the various RF powers at room temperature and post-annealed at different temperatures (170°C, 200°C).

Fig. 6 show the (a) resistivity, (b) carrier density and (c) Hall mobility of the ITO films and ITO:Yb films deposited at room temperature and post-annealed at different temperatures (170°C, 200°C). The resistivity of the films decreased with increasing T_a and increased with increasing RF power. In the case of ITO films, a large change in film resistivity, from 5.89×10^{-4} Ωcm to 2.49×10^{-4} Ωcm, was observed with increasing T_a. The lowest resistivity of 2.49×10^{-4} Ωcm was obtained in the film post-annealed at 200°C, which was due to the increase in carrier density. This result revealed resistivity lower than resistivity (3.96×10^{-4} Ωcm) of amorphous ITO:Ce post-annealed at 200°C[9]. The XRD results confirmed that the ITO films post-annealed above 170°C were polycrystalline structure. Therefore, with increasing film crystallinity, the carrier density of the ITO films increased remarkably by the many carriers generated from the dopant Sn^{4+}.[13] In general, Hall mobility is also affected by the film crystallinity. Therefore, it is expected that Hall mobility is increased with improvement of the film crystallinity. However, Hall mobility of ITO films did not show the large increase with increasing T_a, compared to carrier density. This can be explained by the increase of ionized impurity scattering. That is, change of Hall mobility is offset by both an increase of ionized impurity scattering and a decrease of grain-boundary scattering.

In the case of the ITO:Yb films, the resistivity increased gradually with increasing RF power. The lowest resistivity of 2.62×10^{-4} Ωcm was obtained at a RF power of 120 W and post-annealing at 200°C. The ITO:Yb films had a higher resistivity than the ITO films. This can be explained by the fact that Sn atoms, which act as active donors for free electrons, are not electrically activated in an amorphous structure. The carrier density of the ITO:Yb films decreased with decreasing crystallinity. And also, with increasing Yb content, an increase of resistivity is due to the decrease of Hall mobility, which is attributed to the increase of neutralized impurity scattering. As a result, the amorphous ITO:Yb film had a resistivity of 5.52×10^{-4} Ωcm at an T_a of 170°C.

Fig. 7 shows the optical transmittance measured over the wavelength range of 190-1100 nm for the ITO and ITO:Yb films deposited at (a) room temperature and (b) post-annealed at 170°C. As shown in this figure, all of the films had a high

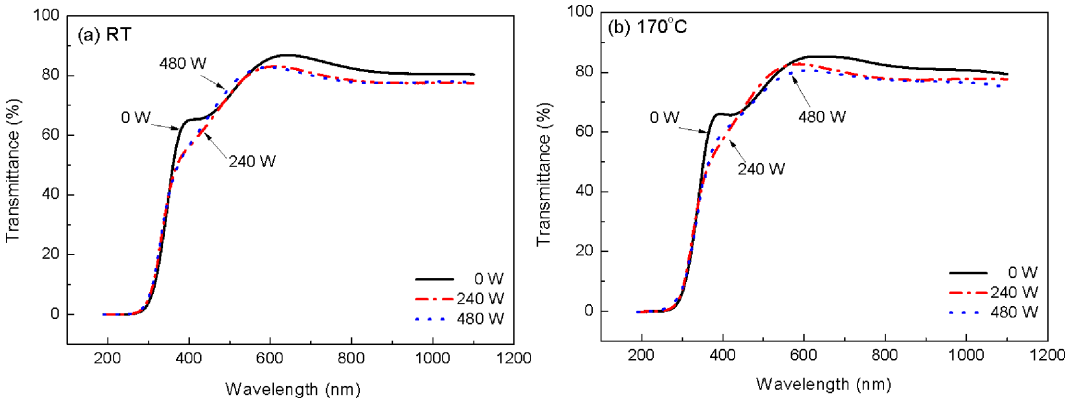

Fig. 7. Transmittance of ITO and ITO:Yb films deposited with the various RF powers at (a) room temperature and (b) post-annealed at 170°C.

transmittance >80% in the visible light region (550 nm), even though transmittance of ITO films slightly decreased with increasing Yb content.

4. Conclusions

ITO and ITO:Yb films were deposited on unheated non-alkali glass substrates by magnetron co-sputtering at various RF powers supplied to the Yb_2O_3 target and post-annealed at different temperatures (170°C, 200°C). The XRD results revealed that the ITO film was polycrystalline structure but the ITO:Yb film was amorphous structure after post-annealed at 170°C, which was attributed to both larger ionic radius of Yb^{3+} and higher bond enthalpy of Yb_2O_3, compared to ITO. However, a polycrystalline structure was observed in all films post-annealed at 200°C. The etching rate of the ITO:Yb films increased with increasing Yb content. The resistivity of the ITO and ITO:Yb films decreased with increasing T_a, which is due to the increase of carrier density. The amorphous ITO:Yb films post-annealed at 170°C showed resistivity of 5.52×10^{-4} Ωcm. On the other hand, the lowest resistivity of ITO (2.49×10^{-4} Ωcm) and ITO:Yb (2.62×10^{-4} Ωcm) was obtained for the polycrystalline films post-annealed at 200°C. The resistivity of the ITO:Yb films increased with increasing Yb content, indicating that the impurity Yb atoms did not contribute to carrier generation. However, it is confirmed that the introduction of Yb atoms improved remarkably the surface morphology, etching rate and patterning property of the ITO film.

Acknowledgments

This research was supported by the R&D project of MKE/KEIT [10039263, Development of window-unified 30 in. touch sensor]. This work was partially supported by the human resources development of the Korea Institute of Energy Technology Evaluation and Planning (KETEP) grant funded by the Korea government, Ministry of Knowledge Economy (No. 20104010100540) and in part by Korea Institute of Materials Science (KIMS).

References

1. Y. H. Jung, E. S. Lee, K. H. Kim, J. Kor. Inst. Surf. Eng., 38 (2005) 150.
2. Z. C. Jin, I. Harmberg, C. G. Granqvist, Thin Solid Films, 64 (1988) 381.
3. P. K. Song, Y. Shigesato, I. Yasui, D. C. Paine, Jpn. J. Appl. Phys., 37 (1998) 1870.
4. J. E. A. van den Meerakker, P. C. Baarslag, W. Walrave, T. J. Vink, Thin Solid Films, 266 (1995) 152.
5. E. Nishimura, M. Ando, K. Onisawa, Jpn. J. Appl. Phys., 35 (1996) 2788.
6. D. C. Paine, T. Whitson, D. Janiac, Jpn. J. Appl. Phy., 85 (1999) 8445.
7. P. K. Song, H. Akao, M. Kamei, Y. Shigesato, Jpn. J. Appl. Phys., 38 (1999) 5224.
8. S. I. Kim, S. H. Cho, P. K. Song, J. Kor. Phys. Soc., 54 (2009) 1297.
9. Y. M. Kang, S. H. Kwon, J. H. Choi, Y. J. Cho, P. K. Song, Thin Solid Films, 518 (2010) 3081.
10. D. Y. Lee, J. R. Lee, P. K. Song, Surf. Coat. Technol., 202 (2008) 5718.
11. T. S. Kim, C. H. Choi, T. S. Jeong and K. H. Shim, J. Kor. Phys. Soc., 51 (2004) 534.
12. C. Guillen, J. Herrero, Vacuum, 80 (2006) 615.
13. Y. Shigesato, D. C. Paine, Appl. Phys. Lett., 62 (1993) 1268.